JACS
JOURNAL OF THE AMERICAN CHEMICAL SOCIETY

Article

pubs.acs.org/JACS

Bespoke Photoreductants: Tungsten Arylisocyanides

Wesley Sattler, Lawrence M. Henling, Jay R. Winkler, and Harry B. Gray*

Beckman Institute, California Institute of Technology, Pasadena, California 91125, United States

Supporting Information

ABSTRACT: Modular syntheses of oligoarylisocyanide ligands that are derivatives of 2,6-diisopropylphenyl isocyanide (CNdipp) have been developed; tungsten complexes incorporating these oligoarylisocyanide ligands exhibit intense metal-to-ligand charge-transfer visible absorptions that are red-shifted and more intense than those of the parent $W(CNdipp)_6$ complex. Additionally, these $W(CNAr)_6$ complexes have enhanced excited-state properties, including longer lifetimes and very high quantum yields. The decay kinetics of electronically excited $W(CNAr)_6$ complexes ($^*W(CNAr)_6$) show solvent dependences; faster decay is observed in higher dielectric solvents. $^*W(CNAr)_6$ lifetimes are temperature dependent, suggestive of a strong coupling nonradiative decay mechanism that promotes repopulation of the ground state. Notably, $^*W(CNAr)_6$ complexes are exceptionally strong reductants: $[W(CNAr)_6]^+/^*W(CNAr)_6$ potentials are more negative than −2.7 V vs $[Cp_2Fe]^+/Cp_2Fe$.

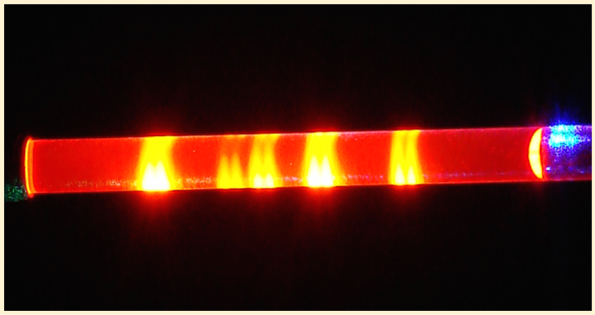

INTRODUCTION

The optical properties of luminescent molecules determine their suitability for applications in solar energy concentration,[1] lighting devices,[2] and biological imaging.[3,4] Luminescence is an indicator of long-lived (>ns) electronic excited states that can initiate chemical reactions unavailable to ground-state molecules.[5−7] This photosensitization capacity of luminophores is finding renewed purpose in solar fuels research,[8,9] as well as inorganic and organic synthesis.[10,11] In this regard, powerfully reducing, organic-solvent soluble, photosensitizers with long excited-state lifetimes are in particular demand.[12] To deliver photosensitizers custom-tailored for targeted applications, we must acquire a deeper understanding of the photophysical properties of luminescent molecules.

In our search for tunable new photosensitizers, we found that $M(CNAr)_6$ complexes of group 6 metals (M = Cr, Mo, and W) are promising candidates, as they absorb strongly in the visible region (400−550 nm) and luminesce with excited-state lifetimes (τ) up to ∼80 ns, increasing when moving down the periodic table.[13,14] Notably, a 2,6-diisopropylphenyl isocyanide (CNdipp)[15] complex, $W(CNdipp)_6$, was shown to be a very strong photoreductant ($\tau \sim 75$ ns and $E°(W^+/^*W^0) = -2.8$ V vs $Cp_2Fe^{+/0}$ in THF; * denotes lowest energy excited state).[16] Rapid photoinduced electron transfer (ET) from $W(CNdipp)_6$ to anthracene ($E° = -2.50$ V in glyme),[17,18] benzophenone ($E° = -2.30$ V in THF)[17] and cobalticenium ion ($E° = -1.35$ V in THF)[17] was observed in THF solutions. Anthracene was an especially interesting case, where both ET and excitation energy transfer (EET) occurred, with the ET/EET ratio tunable by variation of electrolyte ($[^nBu_4N][PF_6]$) concentration.

Encouraged by these findings, we have extended our work to include the synthesis and study of new homoleptic oligoarylisocyanide tungsten complexes that possess even more remarkable spectroscopic, photophysical, and photochemical properties.

RESULTS AND DISCUSSION

Synthesis and Structural Characterization. Increasing the size of the *ortho* substituents (Me to ^{i}Pr) on the arylisocyanide ligands resulted in longer excited-state lifetimes and greater photostabilities for $W(CNAr)_6$ complexes.[14,16] We have now extended our studies to include functionalization at the *para* position of CNdipp. The following methodology allowed for four new oligoarylisocyanides, derivatives of CNdipp, to be synthesized in two steps from a single synthetic intermediate, *N*-formyl-4-bromo-2,6-diisopropylaniline.[19] Suzuki coupling of an arylboronic acid with *N*-formyl-4-bromo-2,6-diisopropylaniline, followed by dehydration with $OPCl_3$ (Scheme 1) afforded the oligoarylisocyanides (Figure 1). CNdippPh, $CNdippPh^{OMe_2}$, and $CNdippPh^{OMe_3}$ are biarylisocyanides, whereas $CNdippPh^{Ph}$ is a terarylisocyanide.

In prior work,[16] we obtained $W(CNAr)_6$ complexes via reduction of WCl_6 with sodium amalgam, Na(Hg), in the presence of free arylisocyanide (similar to the procedure used by Yamamoto and co-workers).[20] Product yields, however, were low (28% for $W(CNdipp)_6$), and purifications were tedious due to tacky, viscous reaction mixtures. We developed an improved synthesis from $WCl_4(THF)_2$[21] (Scheme 2) that results in higher product yields and easier purification. Crystalline samples of red $W(CNAr)_6$ complexes, $W(CNdipp)_6$, $W(CNdippPh)_6$, $W(CNdippPh^{Ph})_6$, W-

Received: October 24, 2014
Published: January 16, 2015

DOI: 10.1021/ja510973h
J. Am. Chem. Soc. 2015, 137, 1198−1205

Scheme 1

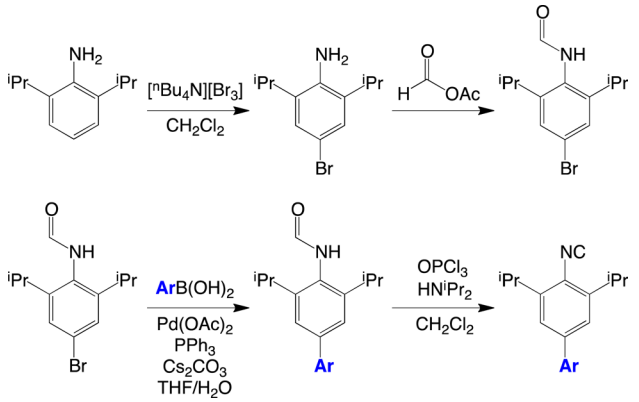

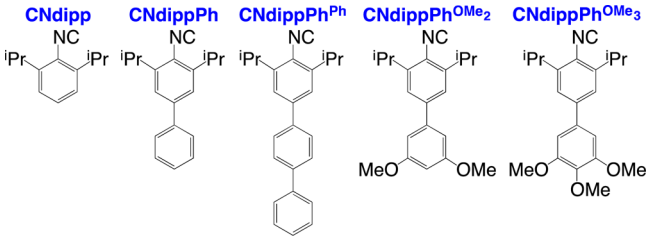

Figure 1. Arylisocyanides.

Scheme 2

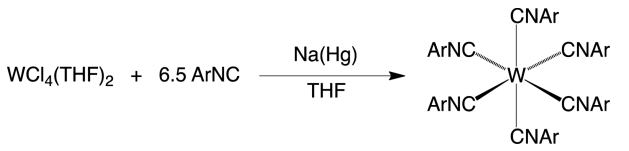

$(CNdippPh^{OMe_2})_6$, and $W(CNdippPh^{OMe_3})_6$, were prepared in yields ranging from 65 to 87%.

The molecular structures of the new $W(CNAr)_6$ complexes were determined by single-crystal X-ray diffraction ($W(CNdippPh^{OMe_2})_6$ shown in Figure 2). Examination of the W−C bond lengths and C−N−C bond angles indicates that the *para* substituents impart little structural change proximal to the tungsten center; selected metrical parameters are provided

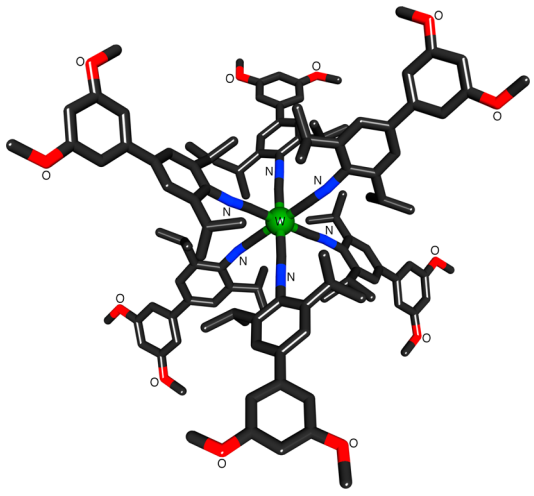

Figure 2. Molecular structure of $W(CNdippPh^{OMe_2})_6$; 45° perspective view; hydrogen atoms removed for clarity.

Table 1. Average Bond Lengths (Å), Bond Angles (deg), and Dihedral Angles (deg) between Aryl Planes of $W(CNAr)_6$ Complexes

$W(CNAr)_6$	d(W−C)	d(C≡N)	∠(C−N−C)	φ_{Ar-Ar}[a]
$W(CNdipp)_6$[b]	2.062	1.176	164.4	n.a.
$W(CNdippPh)_6$[c]	2.045	1.176	171.2	35.0
$W(CNdippPh^{Ph})_6$	2.055	1.171	166.3	33.9[d]
$W(CNdippPh^{OMe_2})_6$	2.056	1.175	169.4	34.3
$W(CNdippPh^{OMe_3})_6$	2.046	1.168	171.7	50.9

[a]Determined by calculating the best least-squares plane through the aryl carbons using the MPLN command in SHELXTL. [b]Data taken from ref 16. [c]Average of two molecules in the asymmetric unit. [d]Average dihedral angle between the two aryl planes proximal to the tungsten center.

in Table 1. Notably, in all of the $W(CNAr)_6$ solid-state structures, the orientation of the π-systems for *trans* arylisocyanide ligands are approximately coplanar (Figure 2). This orientation appears to be enforced by the bulky *ortho* isopropyl groups, as the *trans* arylisocyanide π-systems in $W(CNXy)_6$ (Xy = 2,6-dimethylphenyl) are approximately orthogonal.[22−24] The absorption spectra of the oligoarylisocyanide tungsten complexes are similar to that of $W(CNdipp)_6$ (*vide infra*), not $W(CNXy)_6$. It is noteworthy that $W(CNPh)_6$ has an absorption spectrum similar to that of $W(CNXy)_6$.[14] We suggest that the lowest energy absorption is a property of the fully conjugated orientation (coplanar *trans* arylisocyanide π-systems), which is the lowest energy conformation with *ortho* isopropyl groups.[16] Finally, the average dihedral angles (φ_{Ar-Ar}) of the biaryl rings moieties are ∼35° for $W(CNdippPh)_6$, $W(CNdippPh^{Ph})_6$, and $W(CNdippPh^{OMe_2})_6$ and slightly larger (∼51°) for $W(CNdippPh^{OMe_3})_6$. We attribute the larger dihedral angle in $W(CNdippPh^{OMe_3})_6$ to steric repulsion from two *meta* methoxy groups oriented toward the metal center, whereas only one methoxy group points toward the tungsten center in $W(CNdippPh^{OMe_2})_6$.

The isocyanide stretching frequencies and ^{13}C NMR chemical shifts for the $W(CNAr)_6$ complexes are very similar. The CN vibrations for the complexes are broad and intense, ranging from 1938−1949 cm^{-1} as thin films drop cast from C_6H_6 solutions. In C_6D_6 solutions, the isocyanide ^{13}C NMR chemical shifts are all nearly identical (177.3−177.7 ppm). The free oligoarylisocyanides also exhibit virtually identical isocyanide stretching frequencies (ν(C≡N), 2111−2115 cm^{-1} as thin films drop cast from C_6H_6 solutions and 2118−2119 cm^{-1} in CH_2Cl_2 solutions) and ^{13}C NMR chemical shifts (δ = 169.1−169.3 ppm in $CDCl_3$ solutions).

Absorption and Luminescence Spectra. Absorption and luminescence spectra of $W(CNAr)_6$ complexes in THF solutions are shown in Figure 3 (spectra recorded in toluene and MeCN solutions can be found in the SI). All of the $W(CNAr)_6$ complexes absorb extremely strongly in the visible region, owing to highly allowed metal-to-ligand charge-transfer (MLCT) transitions. Interestingly, the lowest energy MLCT absorption maxima for oligoarylisocyanide complexes are not only red-shifted compared to $W(CNdipp)_6$, as would be expected due to the increased conjugation, but also are more intense. $W(CNdipp)_6$ has a maximum extinction coefficient of ∼9.5 × 10^4 M^{-1} cm^{-1} at 462−464 nm, while values for the biarylisocyanide complexes are roughly 1.3 × 10^5 M^{-1} cm^{-1} at 495−496 nm and ∼1.6 × 10^5 M^{-1} cm^{-1} at 506 nm for $W(CNdippPh^{Ph})_6$. For comparison, the MLCT band in the

DOI: 10.1021/ja510973h
J. Am. Chem. Soc. 2015, 137, 1198−1205

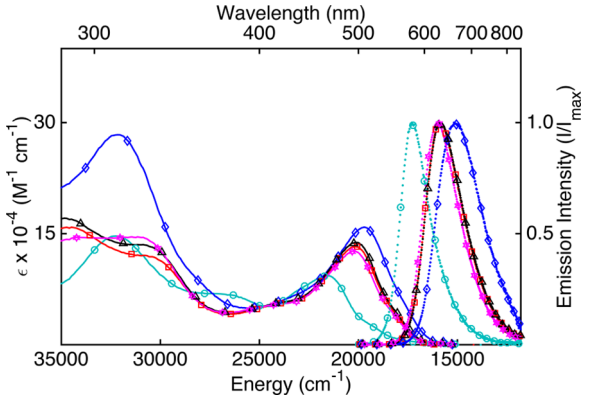

Figure 3. Absorption (solid lines) and emission (dotted lines) spectra of $W(CNdipp)_6$ (cyan/circle), $W(CNdippPh)_6$ (red/square), $W(CNdippPh^{Ph})_6$ (blue/diamond), $W(CNdippPh^{OMe_2})_6$ (black/triangle), and $W(CNdippPh^{OMe_3})_6$ (maroon/hexagram) in THF solutions.

spectrum of $[Ru(bpy)_3]^{2+}$ is much weaker ($\sim 1.45 \times 10^4$ M^{-1} cm^{-1} at 452 nm).[25]

Such intense absorptions in the visible region are remarkable; we suggest that the intensities are due to the high degree of delocalization and spatial overlap between the ground- and excited-state wavefunctions (i.e., there is considerable charge-transfer character in *both* ground and excited states).[26] One may view these MLCT transitions as excitation of an electron from an orbital that has significant tungsten 5dπ and CN π^* character (t_{2g} in idealized O_h symmetry) to one with mainly CN π^* character mixed with tungsten 6p- character (t_{1u} and t_{2u}, O_h). Although there is substantial tungsten 5d delocalization in the ground state, the net dipole is small due to the symmetry of the molecules, as the absorption bands are insensitive to changes in solvent static dielectric constants. Notably, each $W(CNAr)_6$ complex exhibits a shoulder with significant extinction on the low-energy side of the most intense visible MLCT band, which we assign to a series of singlet to triplet transitions.

The most remarkable property of the oligoarylisocyanide complexes is their brilliant luminescence in solution. Under ambient light, toluene solutions of $W(CNdippPh)_6$, $W(CNdippPh^{Ph})_6$, $W(CNdippPh^{OMe_2})_6$, and $W(CNdippPh^{OMe_3})_6$ glow brightly, emitting yellow to red light easily observed by eye. The spectacular photoluminescence observed from the oligoarylisocyanide complexes prompted us to examine their photophysics in more detail.

Luminescence spectra obtained from dilute THF solutions of the $W(CNAr)_6$ complexes are shown in Figure 3. Emission spectra taken in both toluene and THF show similar energy trends as the corresponding absorptions: red-shifting is observed when moving from $W(CNdipp)_6$ to $W(CNdippPh)_6$, $W(CNdippPh^{OMe_2})_6$ and $W(CNdippPh^{OMe_3})_6$, and further to $W(CNdippPh^{Ph})_6$. $W(CNdippPh^{OMe_3})_6$ is slightly blue-shifted from $W(CNdippPh)_6$ and $W(CNdippPh^{OMe_2})_6$, which may be attributed to the electronic influence of (i) the methoxy group at the *para* position and/or (ii) the greater torsion angle between the biaryl planes in $W(CNdippPh^{OMe_3})_6$.

The luminescence bands red-shift and broaden with increasing solvent polarity (full-width at half-maximum values (fwhm) listed in Table 2), which implies that the excited states are able to relax more due to solvent molecule reorientation in higher dielectric media, consistent with a lower-symmetry charge-transfer excited state that has an increased dipole moment compared to the ground state. $*W(CNdippPh^{OMe_2})_6$ and $*W(CNdippPh^{OMe_3})_6$ are distorted significantly in MeCN, apparent by the ~70% increase in luminescence fwhm compared with toluene (Table 2). For comparison, $[Ru(bpy)_3]^{2+}$ has a fwhm of ~2750−3030 cm^{-1} depending on the solvent employed.[27]

It is also interesting to note the difference in energy of the luminescence maximum ($\tilde{\nu}_{max}$) when changing solvent. $W(CNdipp)_6$ has only a 60 cm^{-1} decrease in $\tilde{\nu}_{max}$ when changing from toluene to THF solution, whereas $W(CNdippPh)_6$, $W(CNdippPh^{OMe_2})_6$, and $W(CNdippPh^{OMe_3})_6$ decrease by 220−290 cm^{-1}, and $W(CNdippPh^{Ph})_6$ decreases by 650 cm^{-1}. This trend implies that $W(CNAr)_6$ complexes containing additional aryl groups have greater excited-state dipoles, which are stabilized to a greater degree in more polar solvents.

Photoluminescence quantum yield (ϕ_{PL}, Table 3) measurements were performed under optically dilute conditions by comparison to $[Ru(bpy)_3][PF_6]_2$ in MeCN (ϕ_{PL} = 0.062).[27,28] The oligoarylisocyanide complexes all have ϕ_{PL} values of ~0.4 in toluene solution, in striking contrast to $W(CNdipp)_6$, which has ϕ_{PL} ~ 0.03. Switching from toluene to THF solutions lowers ϕ_{PL} for $W(CNdipp)_6$, $W(CNdippPh)_6$, $W(CNdippPh^{OMe_2})_6$, and $W(CNdippPh^{OMe_3})_6$ by ~50%; and even more dramatically for $W(CNdippPh^{Ph})_6$, where ϕ_{PL} drops by a factor of 6 (Table 3). Finally, $W(CNdippPh^{OMe_2})_6$ and $W(CNdippPh^{OMe_3})_6$ in MeCN solutions have reduced ϕ_{PL} values, 0.01 and 0.02, respectively. These luminescence data lead to the following conclusions about the photophysics of $W(CNAr)_6$ complexes: the excited states of the oligoarylisocyanide complexes are more luminescent than complexes with monoarylisocyanide ligands; addition of methoxy groups to the biaryl ring has little effect; solvent plays an important role in the excited-state decay dynamics; and greater excited-state dipoles relaxed by solvent polarization (increased fwhm values) in more polar solvents decrease ϕ_{PL} values.

Excited-State Decay Kinetics. $*W(CNAr)_6$ lifetimes (τ) were determined in a variety of solvents (Table 3, 2-MeTHF in

Table 2. $W(CNAr)_6$ Emission Maxima (λ_{max} in nm and $\tilde{\nu}_{max}$ in cm^{-1}) and FWHM values (cm^{-1})[a]

	toluene		THF		MeCN	
$W(CNAr)_6$	λ_{max} ($\tilde{\nu}_{max}$)	fwhm	λ_{max} ($\tilde{\nu}_{max}$)	fwhm	λ_{max} ($\tilde{\nu}_{max}$)	fwhm
$W(CNdipp)_6$	575 (17300)	1610	577 (17300)	1750	[b]	[b]
$W(CNdippPh)_6$	617 (16200)	1880	626 (15900)	2250	[b]	[b]
$W(CNdippPh^{Ph})_6$	629 (15800)	1970	656 (15200)	2670	[b]	[b]
$W(CNdippPh^{OMe_2})_6$	618 (16100)	1890	627 (15800)	2280	670 (14700)	3190
$W(CNdippPh^{OMe_3})_6$	612 (16300)	1850	623 (16000)	2180	650 (15200)	3050

[a]Prior to determining emission maxima and fwhm values, the numbers of photons at a given wavelength (λ) were corrected to the wavenumber ($\tilde{\nu}$) scale by using the relationship, $I(\tilde{\nu}) = I(\lambda) \times \lambda^2$.[29] [b]Not soluble in MeCN.

DOI: 10.1021/ja510973h
J. Am. Chem. Soc. 2015, 137, 1198−1205

Table 3. $W(CNAr)_6$ Excited-State Decay Parameters in Toluene, THF, and MeCN[a] Solutions

	toluene				THF			
$W(CNAr)_6$	τ	ϕ_{PL}	k_r (s^{-1})	k_{nr} (s^{-1})	τ	ϕ_{PL}	k_r (s^{-1})	k_{nr} (s^{-1})
$W(CNdipp)_6$	122 ns	0.03	2.3×10^5	8.0×10^6	75 ns	0.01	1.6×10^5	1.3×10^7
$W(CNdippPh)_6$	1.73 μs	0.41	2.4×10^5	3.4×10^5	1.32 μs	0.21	1.6×10^5	6.0×10^5
$W(CNdippPh^{Ph})_6$	1.53 μs	0.44	2.9×10^5	3.7×10^5	350 ns	0.07	1.9×10^5	2.7×10^6
$W(CNdippPh^{OMe_2})_6$	1.65 μs	0.42	2.6×10^5	3.5×10^5	1.20 μs	0.21	1.8×10^5	6.6×10^5
$W(CNdippPh^{OMe_3})_6$	1.83 μs	0.41	2.2×10^5	3.2×10^5	1.56 μs	0.25	1.6×10^5	4.8×10^5

[a]Values for $W(CNdippPh^{OMe_2})_6$ in MeCN are τ = 94 ns, ϕ_{PL} = 0.01, $k_r = 9.6 \times 10^4$ s^{-1}, $k_{nr} = 1.1 \times 10^7$ s^{-1}; values for $W(CNdippPh^{OMe_3})_6$ in MeCN are τ = 210 ns, ϕ_{PL} = 0.02, $k_r = 9.8 \times 10^4$ s^{-1}, $k_{nr} = 4.7 \times 10^6$ s^{-1}.

SI). The oligoarylisocyanide complexes have longer-lived excited states than $W(CNdipp)_6$ (Figure 4 shows luminescence

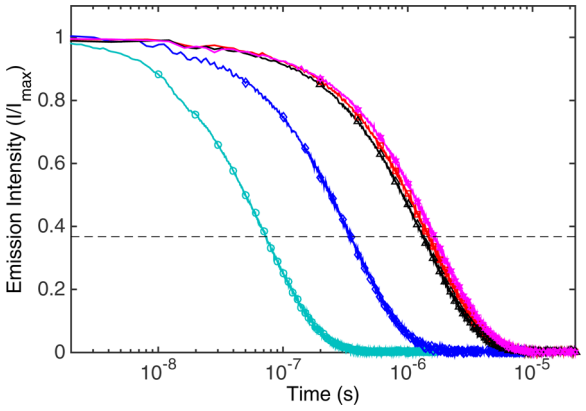

Figure 4. Time-resolved luminescence traces (λ_{ex} = 488 nm, 8 ns pulse) of $W(CNdipp)_6$ (cyan/circle), $W(CNdippPh)_6$ (red/square), $W(CNdippPh^{Ph})_6$ (blue/diamond), $W(CNdippPh^{OMe_2})_6$ (black/triangle), and $W(CNdippPh^{OMe_3})_6$ (maroon/hexagram) in THF solutions. Emission observed at λ_{max} for each complex. The time at which the intensities cross e^{-1} (horizontal dashed line) give the time constants.

decays in THF solutions), and τ values are smaller in more polar solvents. Specifically, in going from toluene to THF solutions, $*W(CNAr)_6$ lifetimes decrease, most dramatically for $W(CNdippPh^{Ph})_6$ (almost 80%). In comparison, τ values for $*W(CNdipp)_6$, $*W(CNdippPh)_6$, $*W(CNdippPh^{OMe_2})_6$, and $*W(CNdippPh^{OMe_3})_6$ decrease by ~15−40%. $*W(CNdippPh^{OMe_2})_6$ and $*W(CNdippPh^{OMe_3})_6$ in MeCN solutions show a pronounced change, where lifetimes drop by close to 90% compared to values in toluene solutions.

The collected data can be analyzed to determine the radiative and nonradiative decay rate constants (k_r and k_{nr}) as shown in eq 1:[30]

$$\tau = \frac{1}{k_r + k_{nr}} \qquad \phi_{PL} = \tau k_r \tag{1}$$

Radiative decay rate constants for $*W(CNAr)_6$ in toluene, THF, and MeCN solutions (Table 3) are fairly constant in each solvent, ranging from 2.2 to 2.9 × 10^5 and 1.6 to 1.9 × 10^5 s^{-1} in toluene and THF solutions, respectively. In MeCN, $*W(CNdippPh^{OMe_2})_6$ and $*W(CNdippPh^{OMe_3})_6$ have slightly smaller k_r values. Conversely, k_{nr} varies greatly, spanning almost 2 orders of magnitude. Thus, nonradiative decay is key in determining $W(CNAr)_6$ excited-state dynamics.

Further analysis of these data lead to the following conclusions. First, and most notable, in a given solvent there is a large decrease (over 1 order of magnitude) in k_{nr} for the oligoarylisocyanide complexes relative to $W(CNdipp)_6$; it is this large decrease that leads to the bright luminescence. In toluene solutions, $*W(CNdippPh)_6$, $*W(CNdippPh^{Ph})_6$, $*W(CNdippPh^{OMe_2})_6$, and $*W(CNdippPh^{OMe_3})_6$ have virtually identical decay kinetics. Interestingly, in THF solution, $*W(CNdippPh^{Ph})_6$ shows faster nonradiative decay; the increase in k_{nr} by about an order of magnitude when changing from toluene to THF is consistent with the larger distortion (larger fwhm) in THF solution (Table 2). Increased distortions in the excited state usually lead to faster nonradiative decay.[31] While this does appear to be the case for each complex when moving to more polar solvents, it is not the general case for the $W(CNAr)_6$ complexes. Specifically, $W(CNdipp)_6$ has the narrowest luminescence profile, implying minor distortions in the excited state; this situation would be expected to produce slow nonradiative decay. The opposite situation occurs, however, where the oligoarylisocyanide complexes exhibit slow nonradiative decay and broader luminescence bands than $W(CNdipp)_6$. $W(CNdippPh^{Ph})_6$ has the fastest radiative decay in both toluene and THF, a finding consistent with the overall greater absorptivity of $W(CNdippPh^{Ph})_6$ compared to the other $W(CNAr)_6$ complexes.[32]

Steady-state and time-resolved luminescence experiments on $W(CNAr)_6$ complexes also were performed at 77 K in toluene and 2-methyltetrahydrofuran (2-MeTHF) glasses. In each case there is sharpening on the high-energy side of the luminescence profile, consistent with hot bands losing intensity at 77 K (SI). E_{00} values estimated from these spectra are given in Table 4. As

Table 4. Ground-State and Excited-State Reduction Potentials (V vs $Cp_2Fe^{+/0}$)

$W(CNAr)_6$	$E°(W^+/W^0)$[a]	E_{00}[b]	$E°(W^+/*W^0)$
$W(CNdipp)_6$	−0.72	2.28	−3.00
$W(CNdippPh)_6$	−0.68	2.12	−2.80
$W(CNdippPh^{Ph})_6$	−0.67	2.08	−2.75
$W(CNdippPh^{OMe_2})_6$	−0.65	2.14	−2.79
$W(CNdippPh^{OMe_3})_6$	−0.65	2.15	−2.80

[a]Room temperature, 0.5 M $[^nBu_4N][PF_6]/CH_2Cl_2$. [b]77 K in 2-MeTHF.

expected, E_{00} values decrease in the order $W(CNdipp)_6 \gg W(CNdippPh^{OMe_3})_6 > W(CNdippPh)_6$, $W(CNdippPh^{OMe_2})_6 > W(CNdippPh^{Ph})_6$. Interestingly, $*W(CNAr)_6$ are significantly longer lived at 77 K but do not follow single exponential decay kinetics as expected for a single emitting excited state (SI). While a single lifetime value does not exist for each $W(CNAr)_6$ complex at 77 K, mean lifetimes can be obtained by integration of the normalized luminescence traces, giving values which range from 5.1−6.1 μs in toluene and 8.2−10.9 μs in 2-MeTHF (see SI, Table S2). At this point, a tentative explanation is that $W(CNAr)_6$ complexes in frozen glasses have multiple static

DOI: 10.1021/ja510973h
J. Am. Chem. Soc. 2015, 137, 1198−1205

confirmations, giving rise to a distribution of excited-state lifetimes. Regardless, these data imply that the faster room temperature process is a thermally activated process (*vide infra*).

Excited-State Decay Pathways. As radiative decay rate constants are generally temperature independent,[32] it follows that increases in lifetimes when going from room temperature to 77 K are due to slower nonradiative decay processes. Temperature dependence in nonradiative decay kinetics implies strong-coupling behavior (considerable displacement along the horizontal axis of one electronic state's potential energy surface with respect to another),[33] where a thermally activated pathway is largely responsible for decay to the ground state. Although additional in-depth variable temperature spectroscopic studies will provide more insight into the decay process (e.g., apparent activation energy, important vibrational frequencies), our finding that the excited-state decay kinetics for $W(CNAr)_6$ complexes are approximately the same in a specific glass at 77 K suggests that a strongly coupled pathway is active for room temperature decay.[34] This type of behavior observed for $[Ru(bpy)_3]^{2+}$ has been attributed to thermal activation to a ligand field (LF) excited state.[35,36]

It is highly unlikely that LF states of $W(CNAr)_6$ complexes are accessible for thermal activation from the $^3T_{1u}$ MLCT excited state. Estimates of the harmonic potential surfaces of the $^1T_{1g}$, $^1T_{2g}$, $^3T_{2g}$, and $^5T_{2g}$ LF states of $W(CNAr)_6$ from $W(CO)_6$ spectroscopic data[37] (the ligand field strength of ArNC is comparable to that of CO)[38] clearly show $E_{FC}(^5T_{2g} \leftarrow {}^1A_{1g}) > 50{,}000\ cm^{-1}$. Calculations of minima on the $W(CO)_6$ potential surfaces place the lowest LF state ($^3T_{1g}$) well above ($E_0 \gg 25{,}000\ cm^{-1}$) the ground state (see SI).[39,40] As luminescence proceeds from an MLCT excited state with $E_0 \sim 18{,}300\ cm^{-1}$, a *lower* estimate (assuming same distortion coordinate) of the activation energy required to populate any LF state would be $>8000\ cm^{-1}$. Our finding that LF states of $W(CNAr)_6$ complexes are not accessible thermally is consistent with the observation that photodissociation does not occur.

As mentioned above, the 77 K excited-state lifetimes of the $W(CNAr)_6$ complexes are ~50% longer in 2-MeTHF than in toluene; if we assume that the lifetimes at 77 K are approximately equal to k_r^{-1} (valid if the quantum yields are close to unity, which appears to be the case for the $W(CNAr)_6$ complexes), then k_r will be ~50% larger in toluene than in 2-MeTHF. Interestingly, comparison to room temperature data in toluene and THF shows a similar trend ($k_r \sim 2.2$–$2.9 \times 10^5\ s^{-1}$ in toluene and 1.6–$1.9 \times 10^5\ s^{-1}$ in THF). We conclude that the transition between the ground state and the emitting state has greater oscillator strength in toluene than in THF/2-MeTHF.

It is apparent that employing oligoarylisocyanides rather than monoarylisocyanides as ligands in $W(CNAr)_6$ complexes has a major impact on nonradiative decay behavior. For each individual complex, ϕ_{PL}, emission fwhm, τ, and k_{nr} are all directly related, implying that more pronounced excited-state distortions in higher dielectric solvents promote nonradiative decay. Addition of methoxy substituents on the distal aryl ring ($W(CNdippPh^{OMe_2})_6$ and $W(CNdippPh^{OMe_3})_6$) imparts higher solubility in polar solvents but has little effect on photophysics in these relatively nonpolar solvents.

Photoredox Reactions. We have demonstrated that $W(CNdipp)_6$ can effect visible light driven reductions of challenging substrates.[16] The oligoarylisocyanide complexes have considerably longer lived excited states, along with favorable ground-state electrochemical properties: cyclic voltammograms of $W(CNAr)_6$ complexes at a platinum working electrode in 0.5 M CH_2Cl_2 solution with $[^nBu_4N][PF_6]$ as the supporting electrolyte (performed under dim lighting conditions inside a nitrogen filled glovebox) exhibit reversible waves at $E^\circ \sim -0.7$ V assigned to W^+/W^0 couples (Table 4). The neutral oligoarylisocyanide complexes are all slightly harder to oxidize (~50 mV shift in E°) than $W(CNdipp)_6$. Similar to $W(CNdipp)_6$ in THF solutions,[16] irreversible oxidation events were observed in CH_2Cl_2 solutions when scanning positive of the W^+/W^0 couple for all of the $W(CNAr)_6$ complexes. No evidence for a W^0/W^- couple was found within the solvent window (−2.3 V).

While the ground-state W^+/W^0 potentials span only ~50 mV for the $W(CNAr)_6$ complexes, the excited-state energies range over ~200 meV (Table 4). The combination of these electrochemical and photophysical data gives estimated excited-state reduction potentials, $E^\circ(W^+/{}^*W^0)$, ranging from −2.7 to −3.0 V, with $W(CNdipp)_6$ being the strongest photoreductant. The W^+/W^0 couple for $W(CNdipp)_6$ is ~200 mV more negative in CH_2Cl_2 than in THF.[16]

Scheme 3

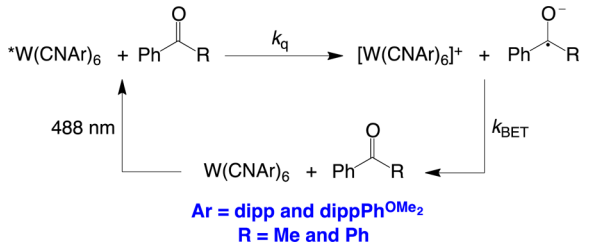

The reactions of $^*W(CNdipp)_6$ and $^*W(CNdippPh^{OMe_2})_6$ with benzophenone and acetophenone[41] are outlined in Scheme 3: $^*W(CNAr)_6$, generated with a 488 nm laser pulse, rapidly reduces benzophenone or acetophenone (second-order rate constant, k_q, Table 5) to give $[W(CNAr)_6]^+$ and a ketyl radical anion.[42] Then the ET quenching products thermally revert to ground-state reactants. As expected, ET from $^*W(CNdippPh^{OMe_2})_6$ is slower than from $^*W(CNdipp)_6$, especially in the case of acetophenone, where the specific quenching rate is attenuated by approximately 2 orders of magnitude, likely attributable to a drop in driving force (Table 4) as well as an effect of the greater size (i.e., greater ET distance) in the reaction with $^*W(CNdippPh^{OMe_2})_6$.

Table 5. ET Quenching Rate Constants (k_q in $M^{-1}\ s^{-1}$) and Reagent (Q) Concentrations Needed to Quench 50% of $^*W(CNAr)_6$

	benzophenone[a]		acetophenone	
$W(CNAr)_6$	k_q	$[Q]_{50\%}$	k_q	$[Q]_{50\%}$
$W(CNdipp)_6$	1.0×10^{10}	1.3 mM	2.2×10^8	0.06 M
$W(CNdippPh^{OMe_2})_6$	2.7×10^9	0.3 mM	2.1×10^6	0.40 M

[a]Data for $W(CNdipp)_6$ and benzophenone taken from ref 16.

Although reactions with $^*W(CNdippPh^{OMe_2})_6$ are slower, its longer lifetime may render it a more versatile photoredox reagent. The concentrations needed to quench equivalent amounts of excited photosensitizers depend both on τ and k_q;

DOI: 10.1021/ja510973h
J. Am. Chem. Soc. 2015, 137, 1198–1205

concentrations needed to quench 50% of $W(CNdipp)_6$ and $W(CNdippPh^{OMe_2})_6$ are listed in Table 5.

Of note, the best known inorganic photosensitizer, ruthenium tris-bipyridine ($[Ru(bpy)_3]^{2+}$ bpy = 2,2′-bipyridine), which has been investigated for over 40 years, has been employed extensively in photoredox catalysis.[10,11,25] The use of $[Ru(bpy)_3]^{2+}$ in organic synthesis is limited by its reducing potential ($E°(Ru^{3+}/*Ru^{2+}) = -1.2$ V vs $Cp_2Fe^{+/0}$ in acetonitrile (MeCN) solutions).[25] MacMillan and co-workers recently demonstrated direct β-functionalization of cyclic ketones with aryl ketones using photoredox and organocatalysis.[12] While these investigators were able directly to reduce diaryl ketones such as benzophenone using *fac*-Ir(ppy)$_3$ (ppy = (2-pyridinyl-κN)phenyl-κ^2C; $E°(Ir^{4+}/*Ir^{3+}) = -2.1$ V vs $Cp_2Fe^{+/0}$ in MeCN solution),[43,44] reduction of aryl alkyl ketones (e.g., acetophenone) was not observed. Electronically excited $W(CNAr)_6$ complexes are capable of reducing such refractory substrates, which should prove to be useful in driving catalytic photoredox reactions.

CONCLUSIONS AND OUTLOOK

Development of a modular synthetic method for oligoaryliso-cyanides has opened the way for the synthesis of new $W(CNAr)_6$ complexes. These complexes, which have extremely rich photophysical and photochemical properties, are sure to find application. Additional experimental and theoretical efforts could shed new light on the electronic structures of their ground and excited states, leading to further photosensitizer customization.

EXPERIMENTAL SECTION

General Considerations. All manipulations and spectroscopic and electrochemical measurments were performed using a combination of glovebox, high vacuum, and Schlenk techniques under a nitrogen or argon atmosphere.[45] Solvents were purified and degassed by standard procedures. NMR spectra were acquired at room temperature unless otherwise noted through the use of Varian spectrometers. ^{1}H NMR chemical shifts are reported in ppm relative to $SiMe_4$ ($\delta = 0$) and were referenced internally with respect to the protio solvent impurity (δ 7.16 for C_6D_5H, 7.26 for $CHCl_3$).[46] $^{13}C\{^1H\}$ NMR spectra are reported in ppm relative to $SiMe_4$ ($\delta = 0$) and were referenced internally with respect to the solvent (δ 128.06 for C_6D_6 and δ 77.16 for $CDCl_3$).[45] Coupling constants are given in hertz. Infrared spectra were recorded either in solution on a Nicolet Avatar 370 DTGS spectrometer or as a thin film from evaporating a benzene solution on the surface of a Bruker ALPHA ATR-IR spectrometer probe (Platinum Sampling Module, diamond, OPUS software package) at 2 cm^{-1} resolution and are reported in cm^{-1}. Samples for transient absorption and room temperature luminescence measurements were prepared in dry, degassed solvents inside a nitrogen-filled glovebox, placed into the cell of a high-vacuum 1 cm path length fused quartz cuvette (Starna Cells), and isolated from atmosphere by a high-vacuum Teflon valve (Kontes). All chemicals were obtained from Aldrich. Acetic formic anhydride (HC(O)OC(O)Me),[47] 2,6-diisopropylphenylisocyanide (dippNC),[16,48] 4-bromo-2,6-diisopropylaniline,[49] and $WCl_4(THF)_2$[21] were prepared as described previously.

Electrochemistry. Electrochemical measurments were made with a Gamry Reference 600 potentiostat/galvanostat using a standard three-electrode configuration. A platinum wire was used as the working electrode. A platinum wire in a fritted (Vycor) glass tube served as the counter electrode. Ag^+/Ag was used as a quasi-reference electrode, and the ferricenium/ferrocene couple (Cp_2Fe^+/Cp_2Fe) served as an internal reference. Measurements were performed at room temperature in either THF solutions with 0.1 M $[^nBu_4N][PF_6]$ as the supporting electrolyte or CH_2Cl_2 solutions with 0.5 M $[^nBu_4N][PF_6]$ as the supporting electrolyte. Sample concentrations were approximately 1 mM.

Photochemical Methods. UV−vis absorption measurements were carried out using a Cary 50 UV−vis spectrophotometer with 1 cm path length quartz cuvettes. Steady-state and time-resolved spectroscopic measurements were carried out in the Beckman Institute Laser Resource Center (California Institute of Technology). Emission and excitation spectra were recorded on a Jobin Yvon Spec Fluorolog-3-11. Sample excitation was achieved via a xenon arc lamp with wavelength selection provided by a monochromator. Right angle luminescence was sorted using a monochromator and detected with a Hamamatsu photomultiplier tube (PMT) with photon counting (PMT model R928P for all spectra with the exception of $W(CNdippPh^{OMe_2})_6$ and $W(CNdippPh^{OMe_3})_6$ in MeCN, where PMT model R2658P was used).

For time-resolved measurements, laser excitation was provided by 8 ns pulses from a Q-switched Nd:YAG laser (Spectra-Physics Quanta-Ray PRO-Series) operating at 10 Hz. The third harmonic was used to pump an optical parametric oscillator (OPO, Spectra-Physics Quanta-Ray MOPO-700) tunable in the visible region to provide laser pulses at 488 nm. Probe light for transient absorption kinetics measurements was provided by a 75-W arc lamp (PTI Model A 1010) that could be operated in continuous wave or pulsed modes. After passing through the sample collinearly with the laser beam, scattered excitation light was rejected by suitable long pass and short pass filters, and probe wavelengths were selected for detection by a double monochromator (Instruments SA DH-10) with 1 mm slits. Transmitted light was detected with a photomultiplier tube (PMT, Hamamatsu R928). The PMT current was amplified and recorded with a GageScope transient digitizer. The data were converted to units of ΔOD (ΔOD = $-\log_{10}(I/I_0)$, where I is the time-resolved probe-light intensity with laser excitation, and I_0 is the intensity without excitation). Data were averaged over approximately 100 shots. All instruments and electronics in these systems were controlled by software written in LabVIEW (National Instruments). Data manipulation was performed with either MATLAB R2012a or MATLAB R2013a (Mathworks, Inc.).

Probe light for transient absorption spectra was provided by flash lamps with either nanosecond or microsecond durations. Probe light was transported via optical fiber and split by a partial reflector. Approximately 70% of the probe light passed through the sample, the remainder directed around the sample as a reference beam. Sample excitation (λ_{ex} = 488 nm) by the laser beam was collinear with the probe light. Sample and reference beams were coupled by optical fibers to a spectrograph and detected using two photodiode arrays (Ocean Optics S1024DW Deep Well Spectrometer), with scattered excitation light rejected by a 488 nm narrow notch filter. The timing synchronization of the laser fire, flashlamp fire, and photodiode array readout was controlled by a series of timing circuits triggered by either a Q-switch advance logic pulse for nanosecond or a laser lamp sync pulse for microsecond, lamp measurements. The photodiode readout was interfaced with a PC via a National Instruments multifunction input/output card. Measurements were made with and without excitation, corrected for dark readout, and corrected for fluorescence when necessary. Difference spectra were averaged over approximately 160 shots. All instruments and electronics in these systems were controlled by software written in LabVIEW (National Instruments).

X-ray Structure Determinations. X-ray diffraction data were collected on either a Bruker Kappa Apex II four circle diffractometer ($W(CNdippPh)_6$, $W(CNdippPh^{OMe_2})_6$, and $W(CNdippPh^{OMe_3})_6$) or a Bruker SMART 1000 three circle diffractometer ($W(CNdippPh^{Ph})_6$). Crystal data, data collection, and refinement parameters are summarized in Table S1. The structures were solved using direct methods and standard difference map techniques and were refined by full-matrix least-squares procedures on F^2 with SHELXTL (Version 2014/2).[50]

DOI: 10.1021/ja510973h
J. Am. Chem. Soc. 2015, 137, 1198−1205

■ ASSOCIATED CONTENT

Supporting Information

Experimental details and crystallographic data in CIF format. This material is available free of charge via the Internet at http://pubs.acs.org.

■ AUTHOR INFORMATION

Corresponding Author

*hbgray@caltech.edu

Notes

The authors declare no competing financial interest.

■ ACKNOWLEDGMENTS

We thank Michael Takase and David VanderVelde for assistance with X-ray and NMR experiments. Discussions with Aaron Rachford, Paul LaBeaume, Jim Thackeray, and Jim Cameron in the early stages of this work were very helpful. The Bruker KAPPA APEX II X-ray diffractometer was purchased via an NSF CRIF:MU award to the California Institute of Technology (CHE-0639094). Our work is supported by the National Science Foundation Center for Chemical Innovation in Solar Fuels (CHE-1305124) and a CCI postdoctoral fellowship to W.S.

■ REFERENCES

(1) (a) Bailey, S. T.; Lokey, G. E.; Hanes, M. S.; Shearer, J. D. M.; McLafferty, J. B.; Beaumont, G. T.; Baseler, T. T.; Layhue, J. M.; Broussard, D. R.; Zhang, Y.-Z.; Wittmershaus, B. P. *Sol. Energy Mater. Sol. Cells* **2007**, *91*, 67−75. (b) Zhao, Y.; Meek, G. A.; Levine, B. G.; Lunt, R. R. *Adv. Optical Mater.* **2014**, *2*, 606−611.

(2) (a) Yersin, H. *Highly Efficient OLEDs with Phosphorescent Materials*; Wiley-VCH: Weinheim, 2008. (b) Yersin, H.; Rausch, A. F.; Czerwieniec, R.; Hofbeck, T.; Fischer, T. *Coord. Chem. Rev.* **2011**, *255*, 2622−2652.

(3) (a) Winkler, J. R.; Gray, H. B. *Chem. Rev.* **2014**, *114*, 3369−3380. (b) Winkler, J. R.; Gray, H. B. *J. Am. Chem. Soc.* **2014**, *136*, 2930−2939. (c) Tran, N.-H.; Nguyen, D.; Dwaraknath, S.; Mahadevan, S.; Chavez, G.; Nguyen, A.; Dao, T.; Mullen, S.; Nguyen, T.-A.; Cheruzel, L. E. *J. Am. Chem. Soc.* **2013**, *135*, 14484−14487. (d) Winkler, J. R.; Nocera, D. G.; Yocom, K. M.; Bordignon, E.; Gray, H. B. *J. Am. Chem. Soc.* **1982**, *104*, 5798−5800.

(4) Lakowicz, J. R. *Principles of Fluorescence Spectroscopy*; Kluwer Academic/Plenum Publishers: New York, 1999.

(5) Leonhardt, H.; Weller, A. *Ber. Bunsenges. Phys. Chem.* **1963**, *67*, 791−795.

(6) Gafney, H. D.; Adamson, A. W. *J. Am. Chem. Soc.* **1972**, *94*, 8238−8239.

(7) Kavarnos, G. J.; Turro, N. J. *Chem. Rev.* **1986**, *86*, 401−449.

(8) Concepcion, J. J.; House, R. L.; Papanikolas, J. M.; Meyer, T. J. *Proc. Natl. Acad. Sci. U.S.A.* **2012**, *109*, 15560−15564.

(9) Gray, H. B.; Maverick, A. W. *Science* **1981**, *214*, 1201−1205.

(10) (a) Schultz, D. M.; Yoon, T. P. *Science* **2014**, *343*, 985. (b) Prier, C. K.; Rankic, D. A.; MacMillan, D. W. C. *Chem. Rev.* **2013**, *113*, 5322−5363. (c) Narayanam, J. M. R.; Stephenson, C. R. J. *Chem. Soc. Rev.* **2011**, *40*, 102−113.

(11) (a) Du, J.; Skubi, K. L.; Schultz, D. M.; Yoon, T. P. *Science* **2014**, *344*, 392−296. (b) Bissember, A. C.; Lundgren, R. J.; Creutz, S. E.; Peters, J. C.; Fu, G. C. *Angew. Chem., Int. Ed. Engl.* **2013**, *52*, 5129−5133. (c) Tucker, J. W.; Stephenson, C. R. J. *J. Org. Chem.* **2012**, *77*, 1617−1622. (d) Creutz, S. E.; Lotito, K. J.; Fu, G. C.; Peters, J. C. *Science* **2012**, *338*, 647−651. (e) Du, J.; Espelt, L. R.; Guzei, I. A.; Yoon, T. P. *Chem. Sci.* **2011**, *2*, 2115−2119. (f) Nicewicz, D. A.; MacMillan, D. W. C. *Science* **2008**, *322*, 77−80. (g) Cano-Yelo, H.; Deronzier, A. *J. Chem. Soc., Perkin Trans. 2* **1984**, 1093−1098.

(12) Petronijević, F. R.; Nappi, M.; MacMillan, D. W. C. *J. Am. Chem. Soc.* **2013**, *135*, 18323−18326.

(13) Mann, K. R.; Cimolino, M.; Geoffroy, G. L.; Hammond, G. S.; Orio, A. A.; Albertin, G.; Gray, H. B. *Inorg. Chim. Acta* **1976**, *16*, 97−101.

(14) Mann, K. R.; Gray, H. B.; Hammond, G. S. *J. Am. Chem. Soc.* **1977**, *99*, 306−307.

(15) The abbreviation dipp for 2,6-diisopropylphenyl will be used in this article, whereas the abbreviation Iph was used in references 14 and 16.

(16) Sattler, W.; Ener, M. E.; Blakemore, J. D.; Rachford, A. A.; Labeaume, P. J.; Thackeray, J. W.; Cameron, J. F.; Winkler, J. R.; Gray, H. B. *J. Am. Chem. Soc.* **2013**, *135*, 10614−10617.

(17) Connelly, N. G.; Geiger, W. E. *Chem. Rev.* **1996**, *96*, 877−910.

(18) Dessy, R. E.; King, R. B.; Waldrop, M. *J. Am. Chem. Soc.* **1966**, *88*, 5112−5117.

(19) Diemer, V.; Chaumeil, H.; Defoin, A.; Fort, A.; Boeglin, A.; Carré, C. *Eur. J. Org. Chem.* **2006**, 2727−2738.

(20) Yamamoto, Y.; Yamazaki, H. *J. Organomet. Chem.* **1985**, *282*, 191−200.

(21) Persson, C.; Andersson, C. *Inorg. Chim. Acta* **1993**, *203*, 235−238.

(22) Lockwood, M. A.; Fanwick, P. E.; Rothwell, I. P. *Organometallics* **1997**, *16*, 3574−3575.

(23) Cambridge Structural Database (Version 5.35). Search performed on May 23, 2014. 3D Search and Research Using the Cambridge Structural Database. Allen, F. H.; ; Kennard, O.; *Chemical Design Automation News*, **1993**, *8*(1), pp 1 and 31−37.

(24) CSD deposition code: NEVSIQ.

(25) Kalyanasundaram, K. *Coord. Chem. Rev.* **1982**, *46*, 159−244.

(26) (a) Mulliken, R. S. *J. Am. Chem. Soc.* **1952**, *74*, 811−824. (b) Mulliken, R. S. *J. Phys. Chem.* **1952**, *56*, 801−822.

(27) Caspar, J. V.; Meyer, T. J. *J. Am. Chem. Soc.* **1983**, *105*, 5583−5590.

(28) Demas, J. N.; Crosby, G. A. *J. Phys. Chem.* **1971**, *75*, 991−1024.

(29) Parker, C. A.; Rees, W. T. *Analyst* **1960**, *85*, 587−600.

(30) The observed radiative rate constant is a lower limit as it is the product of the efficiency of crossing into the emitting state and the radiative rate constant.

(31) Strouse, G. F.; Schoonover, J. R.; Duesing, R.; Boyde, S.; Jones, W. E.; Meyer, T. J. *Inorg. Chem.* **1995**, *34*, 473−487.

(32) Strickler, S. J.; Berg, R. A. *J. Chem. Phys.* **1962**, *37*, 814−822.

(33) Englman, R.; Jortner, J. *Mol. Phys.* **1970**, *18*, 145−164.

(34) Milder, S. J.; Brunschwig, B. S. *J. Phys. Chem.* **1992**, *96*, 2189−2196.

(35) Van Houten, J.; Watts, R. J. *J. Am. Chem. Soc.* **1976**, *98*, 4853−4858.

(36) Durham, B.; Caspar, J. V.; Nagle, J. K.; Meyer, T. J. *J. Am. Chem. Soc.* **1982**, *104*, 4803−4810.

(37) Gray, H. B.; Beach, N. A. *J. Am. Chem. Soc.* **1963**, *85*, 2922−2927.

(38) Hummel, P.; Oxgaard, J.; Goddard, W. A., III; Gray, H. B. *J. Coord. Chem.* **2005**, *58*, 41−45.

(39) Winkler, J. R.; Rice, S. F.; Gray, H. B. *Comments Inorg. Chem.* **1981**, *1*, 47−51.

(40) Nakagawa, I.; Shimanouchi, T. *Spectrochim. Acta* **1962**, *18*, 101−113.

(41) Maekawa, H.; Yamamoto, Y.; Shimada, H.; Yonemura, K.; Nishiguchi, I. *Tetrahedron Lett.* **2004**, *45*, 3869−3872.

(42) Transient absorption studies have been completed for $W(CNdipp)_6$ and benzophenone to demonstrate the formation of ET products. See ref 16.

(43) King, K. A.; Spellane, P. J.; Watts, R. J. *J. Am. Chem. Soc.* **1985**, *107*, 1431−1432.

(44) Flamigni, L.; Barbieri, A.; Sabatini, C.; Ventura, B.; Barigelletti, F. *Top. Curr. Chem.* **2007**, *281*, 143−203.

(45) (a) McNally, J. P.; Leong, V. S.; Cooper, N. J. In *Experimental Organometallic Chemistry*, Wayda, A. L.; Darensbourg, M. Y., Eds.; American Chemical Society: Washington, DC, 1987; Chapter 2, pp 6−23. (b) Burger, B. J.; Bercaw, J. E. In *Experimental Organometallic Chemistry*; Wayda, A. L., Darensbourg, M. Y., Eds.; American Chemical

DOI: 10.1021/ja510973h
J. Am. Chem. Soc. 2015, 137, 1198−1205

Society: Washington, DC, 1987; Chapter 4, pp 79−98. (c) Shriver, D. F.; Drezdzon, M. A. *The Manipulation of Air-Sensitive Compounds*, 2nd ed.; Wiley-Interscience: New York, 1986.
(46) (a) Gottlieb, H. E.; Kotlyar, V.; Nudelman, A. *J. Org. Chem.* **1997**, *62*, 7512−7515. (b) Fulmer, G. R.; Miller, A. J. M.; Sherden, N. H.; Gottlieb, H. E.; Nudelman, A.; Stoltz, B. M.; Bercaw, J. E.; Goldberg, K. I. *Organometallics* **2010**, *29*, 2176−2179.
(47) (a) Huffman, C. W. *J. Org. Chem.* **1958**, *23*, 727−729. (b) Krimen, L. I. *Org. Synth.* **1970**, *50*, 1−3.
(48) (a) Kamer, P. C. J.; Nolte, R. J. M.; Drenth, W. *J. Am. Chem. Soc.* **1988**, *110*, 6818−6825.
(49) Diemer, V.; Chaumeil, H.; Defoin, A.; Fort, A.; Boeglin, A.; Carré, C. *Eur. J. Org. Chem.* **2006**, 2727−2738.
(50) (a) Sheldrick, G. M. *SHELXTL, An Integrated System for Solving, Refining and Displaying Crystal Structures from Diffraction Data*; University of Göttingen: Göttingen, Germany, 1981. (b) Sheldrick, G. M. *Acta Crystallogr.* **2008**, *A64*, 112−122.

DOI: 10.1021/ja510973h
J. Am. Chem. Soc. 2015, 137, 1198−1205